

Mesopause temperatures calculated from the $O_2(a^1\Delta_g)$ twilight airglow emission recorded at Maynooth (53.2°N , 6.4°W)

F. J. Mulligan, J. M. Galligan

Department of Experimental Physics, St. Patrick's College, Maynooth, Co. Kildare, Ireland

Received: 5 July 1994/Revised: 10 October 1994 / Accepted: 10 October 1994

Abstract. Spectra of the $O_2(a^1\Delta_g)$ airglow emission band at $1.27\ \mu\text{m}$ have been recorded during twilight at Maynooth (53.2°N , 6.4°W) using a Fourier transform spectrometer. Synthetic spectra have been generated for comparison with the recorded data by assuming a particular temperature at the emitting altitude, and modelling the absorption of each line in the band as it propagates downward through the atmosphere. The temperature used in generating the synthetic spectra was varied until an optimum fit was obtained between the recorded and synthetic data; this temperature was then attributed to the altitude of the emitting layer. Temperatures derived using this technique for 91 twilight periods over an 18-month period exhibit a strong seasonal behaviour with a maximum in winter and minimum in summer. Results from this study are compared with temperatures calculated from the OH(3,1) Meinel band recorded simultaneously. In winter OH temperatures exceed O_2 values by about 10 K, whereas the opposite situation pertains in summer; this result is interpreted in terms of a possible change in the altitude of the mesopause as a function of season. Estimates of the twilight $O_2(0,0)$ total band intensity indicate that its intensity is lower and that its decay is more rapid in summer than in winter, in agreement with earlier observations.

1 Introduction

Ground-based observations of atmospheric emissions that have a well-defined altitude profile are widely used in studies of the dynamical state of the Earth's upper atmosphere (e.g. Takahashi *et al.*, 1985; Viereck and Deehr, 1989; Taylor *et al.*, 1991). Reports of geophysical parameters determined from ground-based observations of emissions not previously employed (Greet and Jacka, 1989) together with new techniques (Tepley, 1985; Wiens *et al.*, 1991) continue to emerge. In this paper, we report

mesopause temperature values derived from the infrared atmospheric system of $O_2(a^1\Delta_g-^3\Sigma_g)(0,0)$ at $1.27\ \mu\text{m}$, recorded at ground level in Maynooth during twilight. These results are compared with rotational temperatures calculated from the OH(3,1) band recorded simultaneously.

The $O_2(a^1\Delta_g-^3\Sigma_g)(0,0)$ emission is the most intense molecular oxygen feature in the infrared airglow spectrum. This band undergoes resonant self-absorption in the lower atmosphere, which has resulted in many observations being made at high altitudes or from aircraft (Noxon, 1982). The emission is so intense, however, that it penetrates to ground level and may easily be observed in twilight and the early night hours. The earliest ground-based twilight spectra from this band were recorded by Lowe (1969) using a Michelson interferometer with a germanium detector. More recently, Turnbull and Lowe (1983) and Baker *et al.* (1985) have presented spectra recorded at ground level from this band. The fact that the band is overlapped by the (8,5) vibrational-rotational lines of the hydroxyl molecule represents a further complication. The twin difficulties of overlapping OH lines and resonant self-absorption in the lower atmosphere have often meant that the $O_2(0,0)$ band has been neglected as far as deriving meaningful geophysical parameters is concerned.

The altitude profile of this band during twilight and the early night hours has been a subject of much interest recently, since it can be used to derive the daytime mesospheric ozone concentration (McDade *et al.*, 1987; Evans *et al.*, 1988; López-González *et al.*, 1992). McDade *et al.* (1987) concluded from coordinated rocket measurements of $O_2(a^1\Delta_g)$ emission and atomic oxygen densities in an undisturbed night-time atmosphere, that at least two sources of $O_2(a^1\Delta_g)$ excitation must exist in addition to the three-body recombination of atomic oxygen, to account for the observed altitude emission profile. One of these sources, which is thought to account for most of the emission observed below 90 km, is the night-time residual of the very large daytime population of $O_2(a^1\Delta_g)$. The decay time constant of the ($a^1\Delta_g$) state ($\sim 3900\ \text{s}$) (Badger *et al.*, 1965) is very long for an airglow species, and results

in a significant fraction of twilight glow and early nightglow arising from remnant dayglow excitation. López-González *et al.* (1989) have also studied the behaviour of the $O_2(0,0)$ infrared atmospheric band in the middle atmosphere during evening twilight, by considering in detail the different processes governing the production and loss mechanisms of $O_2(a^1\Delta_g)$ near sunset. López-González *et al.* (1992) have presented daytime mesospheric ozone concentrations based on a calculation of the dayglow remnant that is present in the O_2 infrared atmospheric system in the twilight and early night hours.

All the observations reported in this study were recorded during twilight corresponding to solar zenith angles (SZA) approximately between 95° and 105° . López-González *et al.* (1992) presented twilight and early nighttime altitude profiles of the infrared atmospheric system of O_2 measured by several investigators. Profiles recorded for solar zenith angles greater than 110° show the peak emission to occur at an altitude near 89 km (Greer *et al.*, 1986), while those recorded for solar zenith angles less than 95° put the peak emission below 70 km (Llewellyn and Witt, 1977). This increase in the altitude of peak emission is a result of the decay, during twilight, of the large dayglow remnant of the $O_2(a^1\Delta_g)$ emission, which has a daytime maximum near 50 km (Howell *et al.*, 1990). Based on the results of López-González *et al.* (1989), the peak in the $O_2(0,0)$ infrared atmospheric emission profile at $1.27\ \mu\text{m}$ rises from an altitude of ~ 82.5 km, at a solar zenith angle of 95° , to 85 km for a solar zenith angle of 105° . López-Moreno *et al.* (1987) presented results on the altitude distribution of vibrationally excited states of hydroxyl at levels $v = 2$ to $v = 7$, derived from rocket photometry data. Their results show an altitude distribution which is dependent on vibrational level. The lower levels $v = 2, 3$ have peak concentrations centred on 85 km, while the corresponding maxima occur some 5 km higher in the upper levels. McDade (1991) has predicted, however, that the altitude difference between the lowest and highest vibrational levels should not exceed 2 km based on model calculations. The mean altitude profile of the hydroxyl band as reported by Baker and Stair (1988) shows a maximum at about 87 km. The close proximity of the peak emission from the two bands (87 and ~ 84 km for the OH and O_2 , respectively) makes these ideal candidates for an intercomparison of temperature values.

Many investigators have made simultaneous temperature measurements from two distinct altitude levels by observing separate emissions, since Noxon (1978) first compared temperatures derived from the $O_2(b^1\Sigma_g^+ - X^3\Sigma_g^-)(0,1)$ atmospheric band with similar values obtained from the OH(6,2) band centred at 87 km. The $O_2(0,1)$ atmospheric band which originates at an altitude of 95 km is the molecular oxygen emission which has received greatest attention in this respect. Viereck and Deehr (1989) used the same band as Noxon for a comparison of temperatures and band intensities in a study of gravity wave activity in the polar night airglow. Scheer and Reisin (1990) studied the same pair of emission bands at 32° south using a tilting filter photometer and observed a summer enhancement of 15 K in O_2 temperatures which had not previously been reported. Niciejewski and Yee

(1991) used the same band of molecular oxygen, but chose instead the (3,1) band of OH for a comparison of rotational temperatures as part of the Airborne Lidar and Observations of the Hawaiian Airglow (ALOHA-90) campaign. We believe that the work reported here represents the first comparison of temperatures derived from simultaneous ground-based observations of the $O_2(0,0)$ and OH(3,1) bands.

2 Observations and data analysis

Observations were made in the zenith direction at Maynooth (53.2°N , 6.4°W) using a Fourier transform infrared spectrometer supplied by Bomem Inc (Québec, Canada). Evans *et al.* (1970) have noted the futility of making observations in directions other than the zenith to obtain increased intensity via the van Rhijn effect, since any increase in intensity is offset by the decrease in transmission for this band. Our instrument uses a thermoelectrically cooled InGaAs detector, which is sensitive in the wavelength region $1\text{--}1.7\ \mu\text{m}$. This wavelength range has enabled us to record both $O_2(0,0)$ band at $1.27\ \mu\text{m}$, and the OH(3,1) and (4,2) emissions, centred around $1.56\ \mu\text{m}$ simultaneously. An internal He-Ne laser provides accurate data sampling and the instrument has a maximum resolution of $2\ \text{cm}^{-1}$. A complete interferogram is acquired in about 5 s. The field-of-view is $\approx 1.5^\circ$ and typically 50 interferograms are coadded to increase the signal-to-noise ratio. The resulting interferogram is apodized using the Hanning window and the spectra are obtained by calculating the Fourier transform of the apodized interferogram. The relative spectral response of the detector is determined by calibration with a low-intensity source whose area is sufficient to completely fill the field-of-view of the instrument. The calibration of the low-intensity source is traceable to a primary standard and we estimate that radiances calculated on the basis of this source are accurate to $\pm 20\%$. Figure 1 shows a series of spectra recorded near sunset at Maynooth on 16 March 1994. Each spectrum shown is the raw spectrum recorded by the instrument in a 5-min interval and has not been corrected for instrument response. Rayleigh-scattered sunlight dominates the spectra until about 19.06 UT after which the sun is more than 5° below the ground-level horizon and the $O_2(0,0)$ band can be seen clearly. As the sun moves further below the horizon the intensity of the $O_2(0,0)$ band decreases steadily until the spectra become dominated by the OH(8,5) lines which remain relatively constant in intensity throughout the night. Table 1 lists the solar zenith angle for the spectra shown in Fig. 1.

The analysis of the $O_2(0,0)$ spectra for temperature is based on generating a synthetic spectrum which would be observed at ground level, with an assumed temperature at the emission altitude for comparison with the recorded spectrum. We adopted a variation of the method described by Tepley (1985), whereby synthetic spectra are generated at intervals of 1° in the range $150\text{--}300$ K. The temperature corresponding to the synthetic spectrum that best fits the recorded spectrum in the least-squares sense is the value attributed to the emission altitude for that

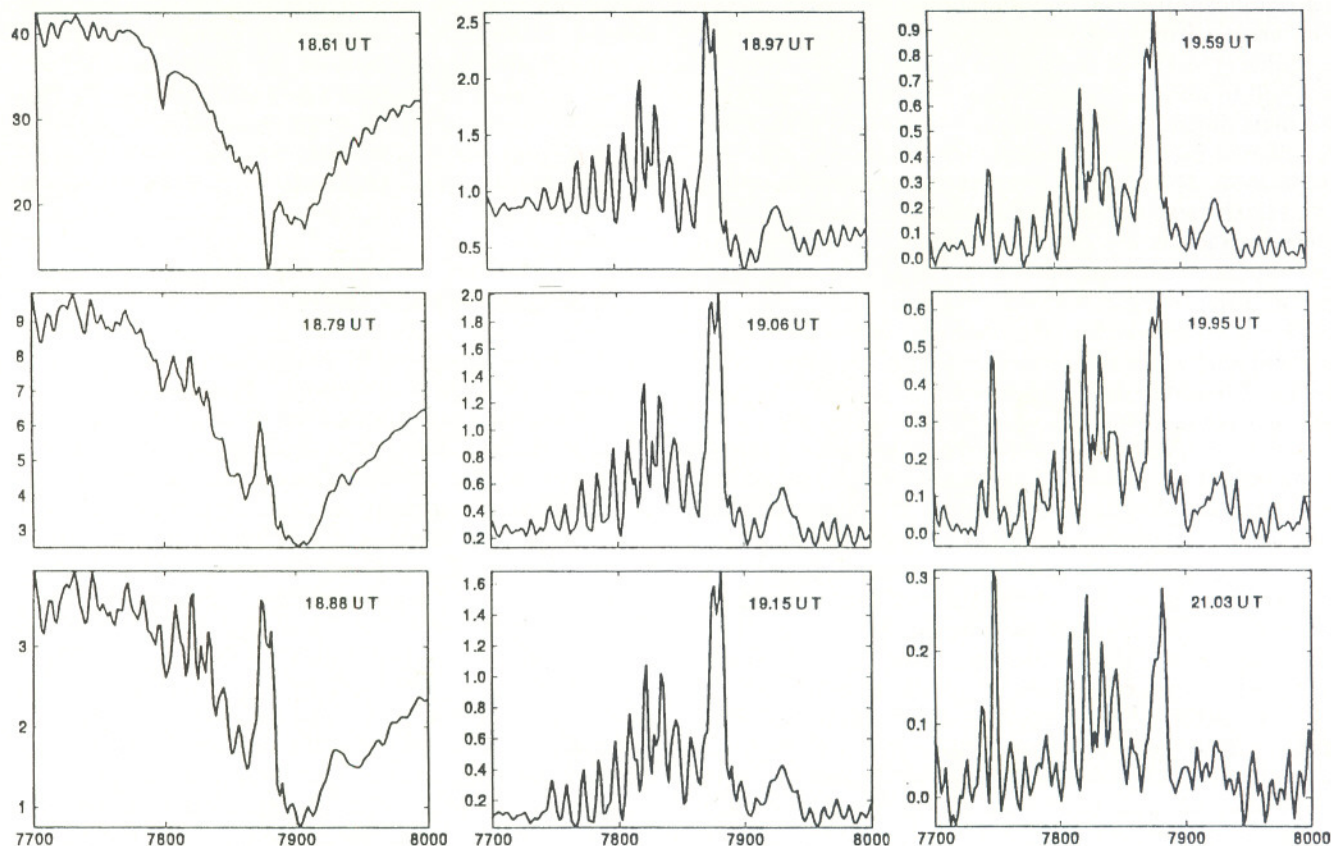


Fig. 1. Series of near-infrared spectra illustrating the development and decay of the $O_2(0,0)$ band during twilight on 16 March 1994 at Maynooth. The abscissa is labelled in cm^{-1} and the ordinate is the signal level recorded by the spectrometer in relative units. Ground-level sunset occurred at 18.48 UT. After 19.06 UT the solar zenith

angle was greater than 95° and the background of Rayleigh-scattered sunlight is negligible, allowing the $O_2(0,0)$ band to stand out clearly in the spectrum. At 19.95 UT, the OH(8,5) lines begin to dominate the spectrum in the interval 7700–8000

spectrum. The technique employed to calculate the synthetic spectrum of $O_2(0,0)$ band in this study follows a method developed by Sue and Baker (1976) for the $O_2(0,1)$ band, and may be summarised in the following three steps:

1. For an assumed temperature at the emission altitude, the relative intensity of enough individual rotational lines to adequately describe the $O_2(0,0)$ band is calculated. Each line is assumed to have a profile determined by Doppler broadening.
2. The transmission of each Doppler-broadened rotational line through the atmosphere from the emission altitude to ground level is calculated.
3. The transmitted spectral lines are then convolved with the appropriate instrument function.

The first step in the generation of a ground-level synthetic spectrum is the calculation of the intensity of a sufficiently large number of individual rotational lines to provide a good description of the $O_2(0,0)$ band at the emission altitude. A total of 108 lines was used to represent the band in this study, which corresponds to 99.8% of the total $O_2(0,0)$ band intensity at $1.27 \mu m$ at temperatures typical of the mesopause. A relative integrated emission intensity has been calculated for each rotational line using the line strength values, S_j , quoted by van Vleck

(1934) for the $O_2(a^1\Delta_g - X^3\Sigma_g)(0,0)$ band. Taking the ratio of the intensity of each line to the intensity sum of all the lines representing the band gives the fractional emission intensity of the line in the band, and removes the need to assign absolute emission intensities. Each line in the band is assumed to have a width determined by Doppler broadening for the temperature selected, since pressure broadening at an altitude of ~ 84 km is negligible.

The effect of atmospheric attenuation on each rotational line in the band has to be determined by considering the loss processes at work between the emission altitude and the recording spectrometer at ground level. Embry (1978) considers five attenuating mechanisms namely, 1. aerosol scattering, 2. aerosol absorption, 3. Rayleigh scattering, 4. continuous absorption and 5. line absorption. The variation in density and pressure of the atmosphere with altitude means that attenuation coefficients for each process also varies with altitude. This feature has been dealt with by considering the atmosphere as a series of horizontally stratified layers, each 1 km in depth, from 50 km to ground level, following the treatment of Evans *et al.* (1970) and Gadsden and Wraight (1975). Above 50 km the atmosphere is considered so tenuous that its effect on the transmission can be neglected.

Table 1. Temperature and O₂(0,0) band intensity estimates for the zenith profiles recorded during twilight on 16 March 1994. The temperature uncertainties are those returned by the simulation process described in the text. Only profiles at times 19.06–19.95 UT would be accepted by the selection criteria described in the text

Time (UT)	Solar zenith angle χ	Rotational temperature (K)	Band intensity (kR)
18.43	89.52°	150 ± 26	-3110.3
18.52	90.32°	150 ± 27	-2164.3
18.61	91.12°	150 ± 28	-1474.0
18.70	91.93°	150 ± 31	-873.3
18.79	92.73°	150 ± 40	-346.3
18.88	93.54°	150 ± 78	-66.6
18.97	94.34°	240 ± 10	172.9
19.06	95.14°	215 ± 5	166.8
19.15	95.94°	209 ± 4	158.7
19.24	96.74°	210 ± 4	137.3
19.33	97.54°	199 ± 5	124.2
19.42	98.34°	202 ± 5	117.4
19.50	99.04°	212 ± 6	103.6
19.59	99.83°	205 ± 8	92.8
19.68	100.62°	211 ± 8	89.0
19.77	101.41°	203 ± 8	81.6
19.86	102.19°	209 ± 8	79.9
19.95	102.96°	210 ± 9	74.5
20.04	103.74°	208 ± 11	71.2
20.13	104.51°	208 ± 10	67.0
20.22	105.27°	212 ± 10	56.0
20.31	106.03°	191 ± 14	55.9
20.40	106.78°	229 ± 13	57.7
20.49	107.53°	241 ± 14	50.2
20.58	108.27°	226 ± 19	44.6
21.03	111.86°	220 ± 39	33.2

Processes 1–3 above are the simplest to deal with; each of these mechanisms is wavelength-dependent as detailed by Elterman and Toolin (1965), but over the wavelength interval encompassing the O₂(0,0) band, each coefficient can be considered constant for the particular altitude layer under consideration. These three mechanisms, therefore, do not alter the shape of the final synthetic spectrum, and could be omitted, from the point of view of determining a temperature at the emission layer. We have included them in our calculations, however, with a view to estimating intensity values for the O₂(0,0) band. The results of Blickensderfer and Ewing (1969) were used to determine a continuous absorption coefficient (process 4 above) for each altitude layer with each coefficient regarded as a constant for a particular rotational line.

Self-absorption of the O₂(0,0) emission by O₂ molecules below the emission altitude contributes by far the greatest fraction of the attenuation of the (0,0) band as it passes through the atmosphere. More significantly, this process alters the shape of an individual rotational line profile as it passes downwards to ground level. Correspondingly, we follow the changes in shape of each rotational line by calculating the intensity at 31 individual data points across the line profile. We have adopted the method of Evans *et al.* (1970), who used the analytical approximation of Whiting (1968) for the variation in optical depth with wave number of a line with both Doppler and Lorentz broadening, to determine the form of each Voigt profile

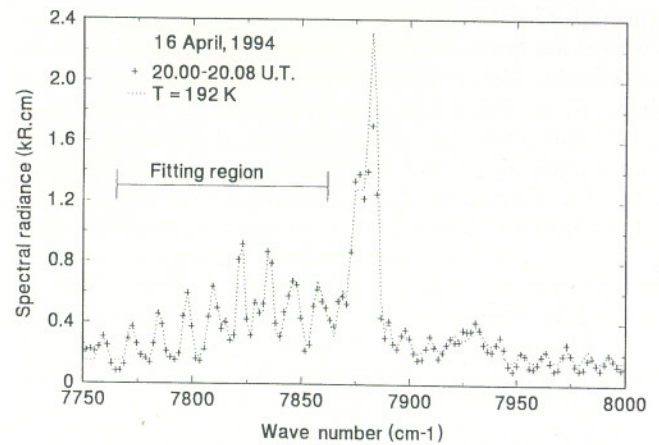


Fig. 2. O₂(0,0) infrared atmospheric band at 1.27 μm and its best-fit synthetic spectrum from 16 April 1994. The fitted theoretical spectrum (.....) for a temperature of 192 ± 3 K is overlaid on the experimental data (+). The fitting region was restricted to 7765–7862 cm⁻¹ to avoid difficulties with the band centre (see text for details) and the Q1(1) line of the OH(8,5) band. The intensity of the entire O₂(0,0) band was estimated to be 84 kR with an absolute uncertainty of about 35%

after transmission through each altitude layer. This has allowed us to calculate an absorption coefficient for each of the 31 points across our original Doppler profile for every layer below 50 km. The U.S. Standard Atmosphere (1976) (Weast *et al.*, 1984) was the model used to provide the values of pressure, temperature and number density in each layer.

In summary, we calculate a loss coefficient, which is the sum of the five attenuation processes described above, at each of the 31 wave number values spanning an individual rotational line for every 1 km layer below 50 km. The loss coefficient at each wave number for that layer is multiplied by the layer thickness and the resulting products are summed over all layers in the transmission path. The transmittance of the path at a particular wave number is calculated from the loss coefficient using a Beer-Lambert-type formula. The transmittance of the line as a whole is then obtained by summing over all 31 wave number values. This process is repeated for each of the 108 lines representing the O₂(0,0) band.

The final step in the production of a ground-level synthetic O₂(0,0) spectrum is the convolution of an instrument function with the 108 lines after atmospheric attenuation processes have been taken into account. The instrument function in our case is the Fourier transform of the Hanning window apodization function, which gives an apodized resolution of 4 cm⁻¹. Figure 2 shows an example of a synthetic spectrum overlaid on an actual spectrum recorded on 16 April 1994. At first glance it can be seen that the gross features of the recorded spectrum are reproduced by the generated curve. A significant disagreement between the two plots occurs near the band centre at 7882 cm⁻¹, where the relative intensity of the synthetic spectrum is much greater than indicated by the recorded spectrum. This is believed to be a result of the close spacing of many individual emission lines at this wave number. The calculation of the transmission,

through the atmosphere, of each of these lines was performed assuming each line behaved independently of the others; this is certainly not true at the band centre, and is believed to account for the disagreement between synthetic and generated intensities in this region. Calculating the attenuation of each $O_2(0,0)$ emission line in the atmosphere, taking account of all other lines is a considerably more complex task and was not attempted in this study.

In calculating a temperature associated with the $O_2(0,0)$ emission, we use a technique similar to that described by Wiens *et al.* (1991) in determining mesopause rotational temperatures from the O_2 atmospheric (0,1) band. A library of synthetic spectra were generated at 1 K intervals in the range 150–300 K for comparison with each recorded spectrum. Each synthetic spectrum was normalized to give a full $O_2(0,0)$ band emission rate of 1 kR following transmission through the atmosphere. The observed spectrum $o(\sigma)$ is considered to be the result of multiplying the synthetic spectrum $s(\sigma)$ by some factor A and adding a constant background B :

$$o(\sigma) = A s(\sigma) + B,$$

where o , s and B are the units of kR/cm^{-1} . We selected a part of the spectrum for the fitting process, so as to minimise difficulties with the vibration-rotation lines of the overlapping OH(8,5) band, and the aforementioned discrepancy between the synthetic and generated spectra at the band centre. The wave number interval chosen was $(7765\text{--}7862)\text{ cm}^{-1}$ as shown in Fig. 2. While this interval includes a number of OH(8,5) lines, in particular the R1(2), R1(3), R2(2), and R2(3) lines, their intensity is quite low in comparison with the O_2 band and they become apparent only at the end of the twilight O_2 period. Nevertheless, we subtract a spectrum recorded, near midnight from each twilight spectrum in an effort to remove these OH lines from the recorded spectrum, thereby assuming that the intensity of the OH lines remain relatively constant during the twilight and night-time periods. The fitting interval, which contains 50 data points in the recorded spectrum, is then compared with the corresponding interval in each synthetic spectrum in the library, and a best fit is obtained in the least-squares sense. The temperature used to generate the synthetic spectrum which corresponds most closely with the recorded spectrum is then assigned to the emission altitude. The fitting procedure requires about 15 s to determine the optimal fit between the recorded and synthetic spectrum using a PC with an 80486 processor running at 33 MHz. Temperatures obtained using this technique for the spectra recorded during the evening of 16 March 1994 are shown in Fig. 3.

In estimating the uncertainty in the recovered temperature, we employ a simulation method similar to that described by Tepley (1985). Random noise was added to a library spectrum at a particular temperature to produce a spectrum with a known signal-to-noise ratio. One hundred of these noisy spectra were generated for each signal-to-noise value; these were analysed in the same way as the sky spectra. The standard deviation on the temperature values calculated for the synthetic spectra was taken as being representative of the error on the temperatures

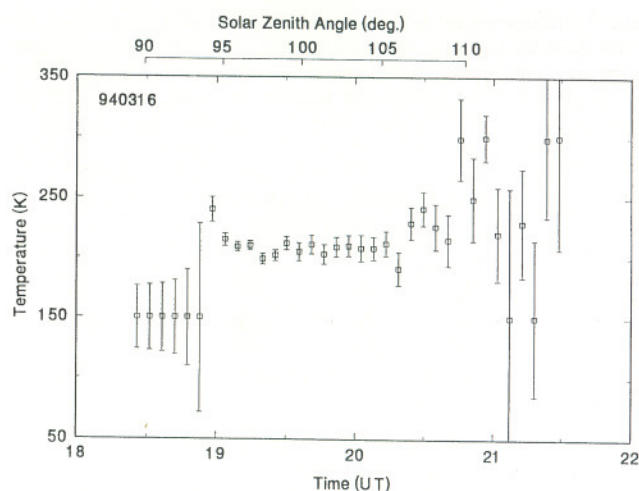


Fig. 3. $O_2(0,0)$ rotational temperatures calculated from twilight $O_2(0,0)$ spectra on 16 March 1994

recorded from the sky for that particular signal-to-noise ratio. This procedure was repeated for a range of signal-to-noise ratios typical of our sky data. Values of temperature uncertainty calculated in this way are in reasonable agreement with the standard deviation of the twilight O_2 rotational temperatures.

The method outlined here can only be used to determine temperatures over a period of about 1–2 h during twilight, when the emission from the $O_2(a^1\Delta_g)$ is sufficiently intense to be observed at ground level. Table 1 lists the values of rotational temperature and intensity for the spectra recorded during the entire twilight period on 16 March 1994. Spectra recorded before the sun reaches a solar zenith angle of 95° are contaminated by scattered sunlight, resulting in a very poor fit between synthetic and recorded data. The fitting process consistently produces high background intensities, and negative intensities of the $O_2(0,0)$ band. Spectra corresponding to the times 18.61–18.88 UT are rejected on the basis that the fitting process predicts negative intensities. Error bars on the earliest of these spectra are not as large as might be expected, because the method used to estimate the uncertainty is weighted according to the intensity of the signal in the fitting region, which is quite large due to scattered sunlight in early twilight. Once the estimated intensity turns positive it decreases steadily as shown in Table 1 and calculated temperatures move away from the lower limit of 150 K set by the library of synthetic spectra. As the intensity of the $O_2(0,0)$ band decreases the uncertainty in the recovered temperatures begins to increase steadily, until a point is reached at a solar zenith angle greater than about 105° , when the temperature values obtained become meaningless. A temperature uncertainty of ± 10 K was chosen, somewhat arbitrarily, as a criterion for accepting a calculated temperature, so that any subjectivity in selecting temperature values might be avoided. Applying these criteria to the data in Fig. 3 results in the acceptance of temperatures corresponding to the times 19.06–19.95 UT. We have used the Elterman and Toolin (1965) atmospheric extinction coefficients as a function of

both wavelength and altitude, to calculate the sensitivity of the recovered temperature values to lower atmosphere variability, and have found that it is less than the 1 K interval used in generating the library of synthetic spectra.

The method employed in fitting a synthetic spectrum to the recorded signal yields a value of the total $O_2(0,0)$ band intensity for each spectrum in addition to the rotational temperature. During a single night the intensity variations follow a generally decreasing trend as expected for this band. Figure 4 illustrates the decay of the emission for two nights in winter and two in summer, plotted as a function of the time after ground-level sunset. In each case the two nights chosen had the greatest intensity in the month. A best-fit exponential curve has been fitted to the data for each twilight period similar to the approach used by Lowe (1969) in an effort to determine the decay constant of the emission. The results of this process are shown in Table 2 and they suggest that the evening twilight intensity is larger and exhibits a slower decay with time in winter in agreement with earlier observations (see e.g. Noxon, 1982, and references therein). Noxon (1982) reported twilight intensities of the $O_2(^1\Delta_g)$ emission band obtained from aircraft measurements in the range 1–2 MR for solar zenith angles greater than 95° at latitudes of 50 – 60° N. Figure 4 shows the intensity values estimated in this study to be in the range 40–200 kR; these estimates are consistent with the results of Noxon, since the transmittance of

the $O_2(0,0)$ band in the spectral interval used in the fitting process is about 10% at a temperature of 200 K. The figure of 10% has been calculated as the ratio of the total intensity in the fitting interval at ground level to that at the emission altitude. Self-absorption of the O_2 band, as it propagates downward through the atmosphere, is by far the greatest attenuator of the incident radiation. The most significant factor determining the magnitude of this attenuation is the temperature assumed at the emission altitude; an increase in temperature of 10 K will result in an increase in transmittance of 0.5% at ground level.

Night-to-night variations in the values of intensity by as much as a factor of 3 have been observed. All the observations reported here were made when sky conditions were clear, as determined by eye, and in meteorological conditions of high pressure. Reimann *et al.* (1992) have attempted to establish characteristic extinction data at visible wavelengths for different meteorological conditions from a long-time photometric study. Since Rayleigh scattering, aerosol absorption and aerosol scattering (processes 1–3 above) contribute only about 10% of the total attenuation of the $O_2(^1\Delta_g)$ band on an average clear day (Elterman and Toolin, 1965), we estimate that variations in $O_2(^1\Delta_g)$ emission intensity arising from variations in atmospheric extinction would not exceed 20%. A more likely source of large night-to-night variations is the occurrence of enhanced auroral activity, resulting in a significant increase in $O_2(^1\Delta_g)$ intensity at our latitude. Noxon (1982) reported observations of enhanced $O_2(^1\Delta_g)$ intensity occurring in coincidence with aurora at latitudes similar to ours. A future study will address the question of correlated variations in O_2 intensity and auroral activity indices.

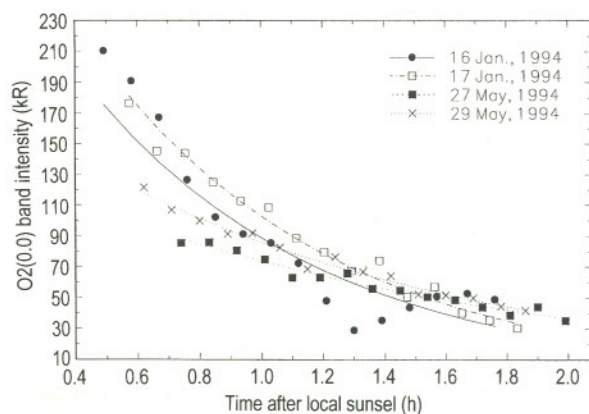


Fig. 4. $O_2(0,0)$ band intensity during twilight for 16/17 January 1994 and 27/29 May 1994 as a function of time after local sunset. The uncertainty associated with the intensity of the band is estimated to be of the order of 35%. The experimental points have been overlaid with the best-fit exponential curve in each case. The decay constant associated with the data for 16/17 January 1994 were 80 ± 13 min and 80 ± 4 min, respectively. The corresponding results for the 27/29 May were 42 ± 3 min and 49 ± 2 min, respectively

Table 2. Decay constants estimated for $O_2(0,0)$ band intensity for two summer and two winter twilight periods

Date	Decay constant (min)
16 January 1994	-80 ± 13
17 January 1994	-80 ± 4
27 May 1994	-42 ± 3
29 May 1994	-49 ± 2

3 Results and discussion

In this study, all spectra were recorded over a 5-min integration time during the evening twilight period. A total of 91 twilight periods were obtained throughout the period January 1993–June 1994, with data in every month except April 1993. All of the spectra were analysed in the manner described above and resulted in typically 8–10 temperature values per twilight period. In winter, the twilight intensity of this band is greater, and it appears to decay more slowly, affording us the opportunity to obtain longer sequences of measurements during this period. Fewer values were obtained during the summer on account of the shorter decay time and lower intensity of the $O_2(0,0)$ band. Temperature values were relatively stable in any one twilight period, but exhibited a well-developed seasonal dependence, with higher temperatures in winter. Figure 5 shows temperature values plotted as a function of the time after ground-level sunset for 16 January 1994, which is typical of winter twilight, and 29 May 1994, which is a representative summer twilight. It is well known that mesopause temperatures exhibit an annual variation, with a maximum in the winter and a minimum in the summer at a latitude of 53° (e.g. Clancy and Rusch, 1989). The generally accepted explanation of this apparent

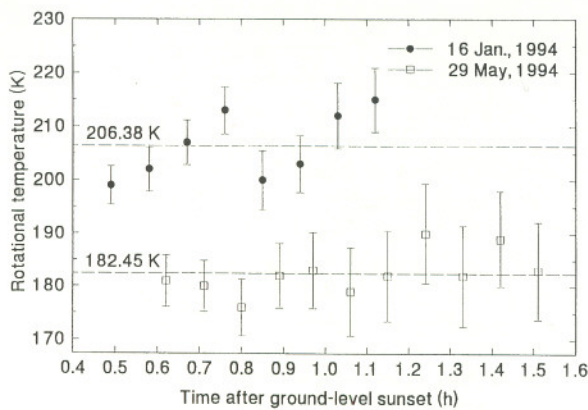


Fig. 5. $O_2(0,0)$ rotational temperatures from 16 January 1994 and 29 May 1994. The twilight averages are shown with a dashed line

inversion is that the cold summer (warm winter) mesopause is maintained through adiabatic cooling (warming) produced by a strong summer-to-winter meridional cell which is driven by breaking vertically propagating gravity waves (Garcia and Solomon, 1985). We felt that the $O_2(0,0)$ results should closely follow the $OH(3,1)$ results due to the proximity of the altitude of peak emission of the two bands. Figure 6 shows the monthly averaged values of $O_2(0,0)$ band temperatures, $T(O_2)$, together with the corresponding $OH(3,1)$ temperatures, $T(OH)$, recorded simultaneously. Rotational temperatures for the $OH(3,1)$ emission were calculated according to the method described by Sivjee and Hamwey (1987), after compensation for detector sensitivity. We have also included in Figure 6 the monthly averaged temperature values reported by Clancy and Rusch (1989) from data recorded by the Solar Mesospheric Explorer (SME) satellite for an altitude of 86.5 km at a latitude of $50^\circ N$ for comparison with the $OH(3,1)$ and $O_2(0,0)$ temperature results. In general, both OH and O_2 temperatures are in very good agreement with the SME data. The correlation between the $O_2(0,0)$ and OH temperature values is remarkable, particularly when one considers that the observing site at Maynooth is only about 60 m above sea level.

Figure 6 shows a clear tendency for $T(OH) > T(O_2)$ during the winter, and $T(OH) < T(O_2)$ during the summer. While the emissions from both bands emanate from altitude layers which have widths in excess of 12 km at half the peak intensities, representative altitudes of 87 km and 84 km were assigned to both the OH and O_2 bands, respectively, in an effort to understand the relative behaviour of the two sets of temperature results. The behaviour of $T(O_2)$ relative to $T(OH)$ might be the result of a change in the altitude of peak emission of either the OH or O_2 bands as a function of season. Baker and Stair (1988) have summarised all of the OH altitude profile measurements since 1950, and while there is considerable variability in the results depending on the OH band selected, there is no evidence of any seasonal variation in the altitude of the OH peak emission. López-Gonzalez *et al.* (1992) have presented altitude profiles of the infrared atmospheric system of O_2 during twilight and early night-time

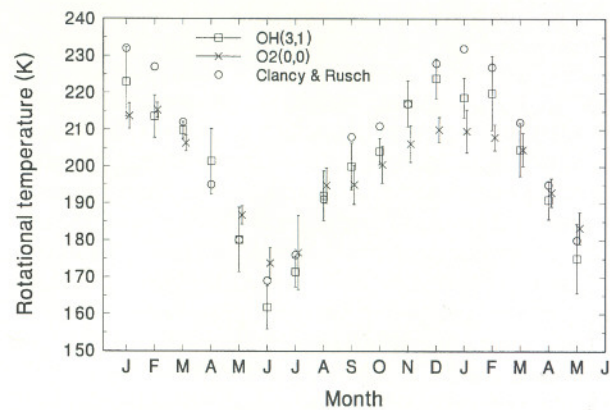


Fig. 6. The mean monthly temperatures calculated from the twilight observations of the $O_2(0,0)$ and $OH(3,1)$ bands during the period January 1993 to June 1994 are shown. Also shown for comparison purposes are the mean monthly temperatures reported by Clancy and Rusch (1989). Temperatures calculated from the $O_2(0,0)$ band appear to be consistently lower in winter and higher in summer than those calculated from the $OH(3,1)$ band. The $O_2(0,0)$ points have been offset by 3 days for clarity

measured by different workers at different times of the year and at the different latitudes and longitudes over a period of 15 years. These data show very little change in the night-time altitude profile of the $O_2(a^1\Delta_g)$ emission between summer and winter in the northern hemisphere. We have been unable to establish whether the twilight altitude profiles exhibit a seasonal variation in the altitude of peak emission, however, due to the shortage of such measurements, and because the measured profiles that have been reported tend to have a more complex structure than the single peaked structure of the later profiles.

Figure 7a and b shows modelled (Hedin, 1991) and measured (Clancy and Rusch, 1989) temperature profiles, respectively, in the region of the mesopause for different seasons. Both panels show the lowest temperatures occurring in summer. The model profiles predict $T(87)$ (the temperature at 87 km) to be less than $T(84)$ in all seasons, with a temperature difference of ~ 5 K in summer and ~ 6.5 K in winter. The altitude of the temperature minimum is lower in summer than at other times of the year. The measurements of Clancy and Rusch (1989) on the other hand generally shows $T(87) > T(84)$ with a maximum difference of 5.6 K in October; exceptions to this trend are found in the months of March, April and November. Although the data of Clancy and Rusch (1989) only covers an altitude region up to a maximum of 90 km, it appears that the altitude of the temperature minimum decreases in winter. The behaviour of $T(O_2)$ relative to $T(OH)$ observed in our data could be most easily explained if the altitude of the mesopause temperature minimum occurred above 87 km in summer ($T(OH) < T(O_2)$), and below 84 km in winter ($T(OH) > T(O_2)$). The idea of a mesopause decreasing in altitude in winter is not inconsistent with the temperature profiles of Clancy and Rusch (1989) shown in Fig. 7b, and our data are in much better agreement with the SME temperature profiles than with the predictions of the MSISE-90 model. Mesopause temperatures calculated from the OH and $O_2(0,0)$ bands

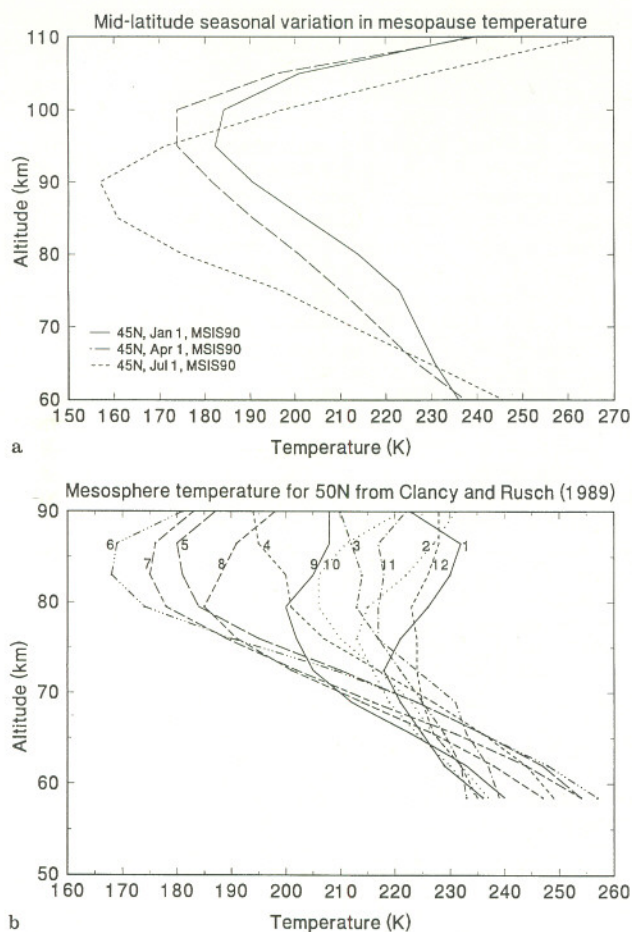


Fig. 7. **a** Seasonal variation of the temperature profile in the region of the mesopause predicted by MSISE-90 (Hedin, 1991) for 45°N. **b** Monthly variation of the temperature profile in the region of the mesopause measured by the Solar Mesospheric Explorer satellite (Clancy and Rusch, 1989) for 50°N

may prove to be a very sensitive indicator of changes in the altitude of the mesopause, as a result of the close proximity of the maximum emission altitude of both bands to the mesopause.

4 Summary

A technique for calculating mesopause temperatures from the $O_2(0,0)$ infrared atmospheric band at 1.27 μm , during twilight and the early night hours has been described. This method has been applied to 91 twilight periods over a period of 18 months. The somewhat limited data set suggests that the O_2 temperatures exhibit an annual behaviour at a latitude of 53°, but with a lower amplitude than in the corresponding temperatures calculated from OH bands. It appears that the technique gives useful results and represents another emission with which to study the complex dynamical behaviour of the mesopause. In addition, estimates of the $O_2(0,0)$ band emission intensity compare favourably with measurements made by earlier workers from aircraft observations. Our results also indicate that the decay of the $O_2(0,0)$ band during

twilight is more rapid in summer than in winter, in agreement with earlier observations. This series of measurements using both O_2 and OH bands is continuing, and it is anticipated that a longer series of data will provide further information on the behaviour of these emissions. The apparent success of the method described here suggests that it should be even more successful at a high-latitude site, where the twilight period can be considerable at certain times of the year.

Acknowledgements. This work was supported by Eolas, the Irish Science and Technology Agency, under grant number RE/176/89. JMG is indebted to Eolas for personal support under grant number SC/91/141. We are grateful to Professor G. A. Ware for providing us with a copy of Embry's Ph.D. thesis, and to an anonymous referee for detailed and helpful comments.

Topical Editor J.-C. Gerard thanks R. Wiens and R. J. Niciejewski for their help in evaluating this paper.

References

- Badger, R. M., A. C. Wright, and R. F. Whitlock, Absolute intensities of the discrete and continuous absorption bands of oxygen gas at 1.26 and 1.065 μm and the radiative lifetime of the 1A_g state of oxygen, *J. Chem. Phys.*, **43**, 4345–4350, 1965.
- Baker, D. J., and A. T. Stair, Jr., Rocket measurements of the altitude distributions of the hydroxyl airglow, *Phys. Sci.*, **37**, 611–622, 1988.
- Baker, D. J., A. J. Steed, G. A. Ware, D. Offerman, G. Lange, and H. Lauche, Ground based atmospheric infrared and visible emission measurements, *J. Atmos. Terr. Phys.*, **47**, 133–145, 1985.
- Blickensderfer, R. P., and G. E. Ewing, Collision-induced absorption spectrum of gaseous oxygen at low temperatures and pressures. I. The $^1A_g \leftarrow ^3\Sigma_g$ -System, *J. Chem. Phys.*, **51**, 873–883, 1969.
- Clancy, R. T., and D. W. Rusch, Climatology and Trends of Mesospheric (58–90 km). Temperatures based upon 1982–1986 SME Limb Scattering Profiles, *J. Geophys. Res.*, **94**, 3377–3393, 1989.
- Elterman, L., and R. B. Toolin, Atmospheric Optics, in *Handbook of Geophysics and Space Environments*, Ed. S. L. Valley, Air Force Cambridge Research Laboratories, Bedford, MA, 1965.
- Embry, U. R., *A study of O_2 infrared radiation in the twilight airglow*, Ph.D. Thesis, Utah State University, Logan, Utah, 1978.
- Evans, W. F. J., I. C. McDade, J. Yuen, and E. J. Llewellyn, A rocket measurement of the O_2 infrared atmospheric (0-0) band emission in the dayglow and a determination of the mesospheric ozone and atomic oxygen densities, *Can. J. Phys.*, **66**, 941–946, 1988.
- Evans, W. F. J., H. C. Wood, and E. J. Llewellyn, Transmission of the infrared oxygen emission at 1.27 μm in the atmosphere, *Can. J. Phys.*, **48**, 747–752, 1970.
- Gadsden, M., and P. C. Wraith, Atmospheric transmission of the 1.27 micron band of oxygen, *J. Atmos. Terr. Phys.*, **37**, 287–296, 1975.
- Garcia, R. R., and S. Solomon, The effect of breaking gravity waves on the dynamics and chemical composition of the mesosphere and lower thermosphere, *J. Geophys. Res.*, **90**, 3850–3868, 1985.
- Greer, R. G. H., D. P. Murtagh, I. C. McDade, P. H. G. Dickinson, L. Thomas, D. B. Jenkins, J. Stegman, E. J. Llewellyn, G. Witt, D. J. MacKinnon, and E. R. Williams, Eton 1: a data base pertinent to the study of energy transfer in the oxygen nightglow, *Planet. Space Sci.*, **34**, 771–778, 1986.
- Greet, P., and F. Jacka, Observations of the sodium layer using a Fabry-Perot spectrometer: twilight temperature variations, *J. Atmos. Terr. Phys.*, **51**, 91–99, 1989.
- Hedin, A. E., Extension of the MSIS thermospheric model into the middle and lower atmosphere, *J. Geophys. Res.*, **96**, 1159–1172, 1991.
- Howell, C. D., D. V. Michelangeli, M. Allen, Y. L. Yung, and R. J. Thomas, SME observations of $O_2(^1A_g)$ nightglow: an assessment of the chemical production mechanisms, *Planet. Space Sci.*, **38**, 529–537, 1990.

- Llewellyn, E. J., and G. Witt, The measurement of ozone concentrations at high latitude during the twilight, *Planet. Space Sci.*, **25**, 165, 1977.
- López-González, M. J., J. J. López-Moreno, M. A. López-Valverde, and R. Rodrigo, Behaviour of the O_2 infrared atmospheric (0-0) band in the middle atmosphere during evening twilight and at night, *Planet. Space Sci.*, **37**, 61–72, 1989.
- López-González, M. J., J. J. López-Moreno, and R. Rodrigo, The Altitude Profile of the Infrared Atmospheric System of O_2 in Twilight and Early Night: Derivation of Ozone Abundances, *Planet. Space Sci.*, **40**, 1391–1397, 1992.
- López-Moreno, J. J., R. Rodrigo, F. Morena, M. López-Puertas, and A. Molina, Altitude distribution of vibrationally excited states of atmospheric hydroxyl at levels $v = 2$ to $v = 7$, *Planet. Space Sci.*, **35**, 1029–1038, 1987.
- Lowe, R. P., Interferometric spectra of the Earth's airglow (1.2 to 1.6 μm). *Phil. R. Trans. Soc., London, Series A*, **264**, 163–169, 1969.
- McDade, I. C., E. J. Llewellyn, R. G. H. Greer, and D. P. Murtagh, Eton 6: A Rocket Measurement of the O_2 Infrared Atmospheric band in the Nightglow, *Planet. Space Sci.*, **35**, 1541–1552, 1987.
- McDade, I. C., The altitude dependence of the OH($X^2\Pi$) vibrational distribution in the nightglow: some model expectations, *Planet. Space Sci.*, **39**, 1049–1057, 1991.
- Niciejewski, R. J., and J. H. Yee, Airglow rotational temperature measurements during the ALOHA-90 campaign, *Geophys. Res. Lett.*, **18**, 1353–1356, 1991.
- Noxon, J. F., Effect of internal gravity waves upon night airglow temperatures, *Geophys. Res. Lett.*, **5**, 25–27, 1978.
- Noxon, J. F., A global study of $O_2(^1\Delta_g)$ airglow: day and twilight, *Planet. Space Sci.*, **30**, 545–557, 1982.
- Reimann, H.-G., G. Ossenkopf, and S. Beyersdorfer, Atmospheric extinction and meteorological conditions: a long time photometric study, *Astron. Astrophys.*, **265**, 360–369, 1992.
- Scheer, J., and E. R. Reisin, Rotational temperatures for OH and O_2 airglow bands measured simultaneously from El Leoncito ($31^\circ 48'S$), *J. Atmos. Terr. Phys.*, **52**, 47–57, 1990.
- Sivjee, G. G., and R. M. Hamwey, Temperature and chemistry of the polar mesopause OH, *J. Geophys. Res.*, **92**, 4663–4672, 1987.
- Sue S.-C., and D. J. Baker, Computer-aided estimates of the rotational temperature of O_2 in the mesosphere, Air Force Geophysics Laboratory Report, *AFGL-TR-76-0212*, 1976.
- Takahashi, H., P. P. Batista, Y. Sahai, and B. R. Clemesha, Atmospheric wave propagations in the mesopause region observed by the OH(8, 3) band, NaD, $O_2A(8645\text{ \AA})$ band and OI 5577 \AA nightglow emissions, *Planet. Space Sci.*, **33**, 381–384, 1985.
- Taylor, M. J., P. J. Espy, D. J. Baker, R. J. Sica, P. C. Neal, and W. R. Pendleton Jr., Simultaneous intensity, temperature and imaging measurements of short-period wave structure in the OH nightglow emission, *Planet. Space Sci.*, **39**, 1171–1188, 1991.
- Tepley, C. A., A nonlinear least-squares approach to the analysis of $O_2(0-1)$ atmospheric band emissions, *Ann. Geophysicae*, **3**, 177–180, 1985.
- Turnbull, D. N., and R. P. Lowe, Vibrational population distribution in the hydroxyl night airglow, *Can. J. Phys.*, **61**, 244–250, 1983.
- van Vleck, J. H., Magnetic dipole radiation and the atmospheric absorption bands of oxygen, *Ap. J.*, **80**, 161–170, 1934.
- Viereck, R. A., and C. S. Deehr, On the Interaction Between Gravity-Waves and the OH Meinel (6-2) and the O_2 Atmospheric (0-1) Bands in the Polar Night Airglow, *J. Geophys. Res.*, **94**, 5397–5404, 1989.
- Weast, R. C., J. A. Astle, and H. B. Beyer, *Handbook of Chemistry and Physics*, 64th ed., CRC Press, Florida, 1984.
- Whiting, E. E., An empirical approximation to the Voigt profile, *J. Quant. Spectrosc. Radiat. Transfer.*, **8**, 1379–1384, 1968.
- Weins, R. H., S.-P. Zhang, R. N. Peterson, and G. G. Shepherd, MORTI: A mesopause oxygen rotational temperature imager, *Planet. Space Sci.*, **39**, 1363–1375, 1991.